AFRL-RX-WP-TP-2011-4293

THE DUALITY OF FRACTURE BEHAVIOR IN A Ca-BASED BULK-METALLIC GLASS (PREPRINT)

Gongyao Wang and Peter K. Liaw

The University of Tennessee

Oleg N. Senkov

UES, Inc.

Daniel B. Miracle

Metals Branch
Metals, Ceramics, and NDE Division

JULY 2011

Approved for public release; distribution unlimited.

See additional restrictions described on inside pages

STINFO COPY

AIR FORCE RESEARCH LABORATORY
MATERIALS AND MANUFACTURING DIRECTORATE
WRIGHT-PATTERSON AIR FORCE BASE, OH 45433-7750
AIR FORCE MATERIEL COMMAND
UNITED STATES AIR FORCE

REPORT DOCUMENTATION PAGE

Form Approved
OMB No. 0704-0188

1. REPORT DATE *(DD-MM-YY)*	2. REPORT TYPE	3. DATES COVERED *(From - To)*
July 2011	Journal Article Preprint	01 July 2011 – 01 July 2011

4. TITLE AND SUBTITLE
THE DUALITY OF FRACTURE BEHAVIOR IN A Ca-BASED BULK-METALLIC GLASS (PREPRINT)

5a. CONTRACT NUMBER
In-house

5b. GRANT NUMBER

5c. PROGRAM ELEMENT NUMBER
62102F

6. AUTHOR(S)
Gongyao Wang and Peter K. Liaw (The University of Tennessee)
Oleg N. Senkov (UES, Inc.)
Daniel B. Miracle (AFRL/RXLM)

5d. PROJECT NUMBER
4347

5e. TASK NUMBER
20

5f. WORK UNIT NUMBER
LM10512P

7. PERFORMING ORGANIZATION NAME(S) AND ADDRESS(ES)

The University of Tennessee
Department of Materials Science and Engineering
Knoxville, TN 37996

UES, Inc.
Dayton, OH 45432-1894

Metals Branch (AFRL/RXLM)
Metals, Ceramics, and NDE Division
Air Force Research Laboratory, Materials and Manufacturing Directorate
Wright-Patterson Air Force Base, OH 45433-7750
Air Force Materiel Command, United States Air Force

8. PERFORMING ORGANIZATION REPORT NUMBER
AFRL-RX-WP-TP-2011-4293

9. SPONSORING/MONITORING AGENCY NAME(S) AND ADDRESS(ES)
Air Force Research Laboratory
Materials and Manufacturing Directorate
Wright-Patterson Air Force Base, OH 45433-7750
Air Force Materiel Command
United States Air Force

10. SPONSORING/MONITORING AGENCY ACRONYM(S)
AFRL/RXLM

11. SPONSORING/MONITORING AGENCY REPORT NUMBER(S)
AFRL-RX-WP-TP-2011-4293

12. DISTRIBUTION/AVAILABILITY STATEMENT
Approved for public release; distribution unlimited.

13. SUPPLEMENTARY NOTES
PAO Case Number: 88ABW 2010-2662; Clearance Date: 18 May 2010. Document contains color.
Journal article submitted to the *Metallurgical and Materials Transactions A.*

14. ABSTRACT
$Ca_{65}Mg_{15}Zn_{20}$ bulk-metallic glass (BMG) exhibited a typical brittle fracture behavior during compressive loading at room temperature. Samples exploded into many small pieces after elastic deformation, and no macroscopic plasticity was observed. The fracture surface demonstrated multiple fracture patterns, including typical metallic-glass vein patterns and glass mirror, mist, and hackle patterns. These observations show that Ca-based BMGs are subjected to multiple brittle fracture modes under compressive loading. Periodic nanoscale corrugations were found in the hackle region, which may indicate local plasticity for the brittle fracture.

15. SUBJECT TERMS
$Ca_{65}Mg_{15}Zn_{20}$, bulk-metallic glass (BMG), elastic deformation, macroscopic plasticity

16. SECURITY CLASSIFICATION OF: a. REPORT	b. ABSTRACT	c. THIS PAGE	17. LIMITATION OF ABSTRACT:	18. NUMBER OF PAGES	19a. NAME OF RESPONSIBLE PERSON (Monitor) / 19b. TELEPHONE NUMBER *(Include Area Code)*
Unclassified	Unclassified	Unclassified	SAR	20	Jonathan E. Spowart / N/A

The Duality of Fracture Behavior in a Ca-based Bulk-Metallic Glass

Gongyao Wang[2], Peter K. Liaw[2], Oleg N. Senkov[1,3], and Daniel B. Miracle[1]

[1] Air Force Research Laboratory, Materials and Manufacturing Directorate, Wright-Patterson AFB, OH 45433, U.S.A.

[2] Department of Materials Science and Engineering, The University of Tennessee, Knoxville, TN 37996, U.S.A.

[3] UES, Inc., Dayton, OH 45432-1894, U.S.A.

ABSTRACT

$Ca_{65}Mg_{15}Zn_{20}$ bulk-metallic glass (BMG) exhibited a typical brittle fracture behavior during compressive loading at room temperature. Samples exploded into many small pieces after elastic deformation, and no macroscopic plasticity was observed. The fracture surface demonstrated multiple fracture patterns, including typical metallic-glass vein patterns and glass mirror, mist, and hackle patterns. These observations show that Ca-based BMGs are subjected to multiple brittle fracture modes under compressive loading. Periodic nanoscale corrugations were found in the hackle region, which may indicate local plasticity for the brittle fracture.

INTRODUCTION

Ca-based bulk-metallic glasses (BMGs) have low density (~ 2.0 g/cm^3), low Young's modulus (~ 20 - 30 GPa), low shear modulus (~ 8 - 15 GPa), low glass-transition temperature (T_g ~ 100 °C - 190 °C), low crystallization temperature (T_x ~ 130 °C - 240 °C), and a wide super-cooled

liquid temperature range ($\Delta T_{xg} = T_x - T_g \approx 30 - 80$°C) [1-3]. In addition, Ca-based BMGs have very good glass-forming ability (GFA) and are based on two simple metals, Ca and Mg [3]. Since first Ca-based BMGs were successfully synthesized [4,5], numerous Ca-based BMG systems have been discovered and studied [6-12]. The elastic modulus of Ca-based BMGs is comparable to the modulus of human bones and Ca, Mg, and Zn are biocompatible. These features make Ca-Mg-Zn-based alloys attractive for biomedical applications [2, 3, 13].

Brittleness at temperatures well below T_g is a common feature of many metallic glasses, such as Zr-, Cu-, Mg-, and Fe- based BMGs [14]. Their brittleness is generally explained by limited deformation carriers that can accommodate the loading conditions, such as linear and planar defects, as well as the absence of strain hardening in amorphous structures [15]. Ca-based BMGs are extremely brittle at room temperature [1, 15, 16]. During compression testing of a $Ca_{65}Mg_{15}Zn_{20}$ (atomic percent) BMG, many thin pieces were observed to shed progressively from free surfaces of samples due to splitting fracture, which eventually exploded into numerous small pieces in the final catastrophic failure [15, 16].

A good understanding of the fracture behavior is critically important for the application of Ca-based BMGs. The unusual, catastrophic failure of Ca BMGs makes it difficult to study the fracture mechanisms that operate during the early stages of failure. In the current paper, the fracture modes are characterized on fracture surfaces produced by interrupted compressive loading of a $Ca_{65}Mg_{15}Zn_{20}$ BMG, and the associated failure mechanisms are discussed.

EXPERIMENT

The $Ca_{65}Mg_{15}Zn_{20}$ (atomic percent, at. %) BMG alloy was fabricated by induction melting pure elements (99.9% weight percent) in a water-cooled copper susceptor in an argon

atmosphere. The prepared alloy was subsequently placed in a quartz crucible with a 2-mm diameter hole at the bottom, induction melted in an argon atmosphere, and injected into a water-cooled copper mold with a 15 mm × 15 mm × 4 mm cavity [1-2]. X-ray diffraction and differential scanning calorimetry (DSC) were used to assess the structure of the 4-mm-thick plates produced. The plates were cut into 4 × 4 × 4 mm^3 samples for compression experiments. Each side of these samples was polished to a 600-SiC-grit-surface finish using a polishing fixture (South Bay Technologies, San Clemente, CA) to keep the sides parallel and perpendicular.

A computer-controlled servohydraulic-testing machine (MTS Systems Corporation, Eden Praire, MN) was employed to conduct the compression tests. The load frame was aligned prior to use. The compression experiments were performed at room temperature under displacement control with an initial strain rate of 10^{-4} s^{-1}. Tungsten-carbide spacers were employed above and below the specimen to prevent the deformation of the pushrods during the compression experiments. Compression loading was stopped immediately after spallation was first observed in the sample, and before the catastrophic, explosive failure observed in the earlier study [15]. In general, 3-4 primary shear or split fracture planes can be observed. Fracture surfaces were characterized by a Leo 1526 scanning electron microscopy (SEM) (LEO Electron Microscopy Ltd., Cambridge, England) immediately after testing to avoid oxidation. Moreover, the angle between the fracture plane and loading direction was measured.

RESULTS AND DISCUSSION

The plates produced were found to be fully amorphous in the as-cast condition [2], and detailed mechanical properties of the $Ca_{65}Mg_{15}Zn_{20}$ BMG have been reported previously [15]. A relatively flat fracture plane with a large angle of approximately 35° with respect to the loading

axis was covered by vein patterns (Figure 1), which are the typical BMG shear-fracture feature. The vein structure has been widely observed and is generally attributed to the significant increase in the temperature in shear bands during the deformation of metallic glasses [17-18]. This feature is consistent with the reported results for many other metallic glasses, which demonstrate that the compressive fracture of metallic glasses does not occur along the plane of the maximum shear stress, and the compressive fracture angle is less than 45° [19-20]. Although the aspect ratio of the current sample is 1, the fracture behavior may not change with the aspect ratio when it is larger than 0.75 [21]. Only specimens with the aspect ratios equal to and smaller than 0.75 exhibit an excellent compressive ductility due to the constraint on the compressive deformation of BMGs [21]. The size of vein patterns varies significantly along the perpendicular direction to the crack propagation, such as from A to B in Figure 1(a). Figure 1(b) shows the elongated cellular vein structure at high magnification. This characteristic vein in BMGs may indicate the relatively ductile local fracture [14]. Vein patterns in BMGs also seem to indicate a pre-melting state of the material at the shear failure surfaces. These facts indicate that the Ca-based BMG exhibits localized shear bands and local plasticity, while it lacks a global shear band and macroscopic plasticity. The width of the dimple vein structure is up to 13.2 μm in the current Ca-based BMG.

Conchoidal fracture morphologies occurred during the fracture of the $Ca_{65}Mg_{15}Zn_{20}$ BMG in the present study. Conchoidal fracture was generally found on fracture planes that locally appear to be inclined by about 0 - 20° to the direction of the applied load. This fracture surface produced the splitting fracture mode in the $Ca_{65}Mg_{15}Zn_{20}$ BMG [15, 16]. Figure 2(a) presents the very smooth mirror region near the fracture origin, the mist region, which transitions from mirror to hackle regions, and the hackle region with radiating ridges and valleys [Figure 2(b)]. The smooth

mirror surface produces in the initial fracture region. Then, a rougher surface known as mist is created when the crack accelerates and becomes unstable. Moreover, this instability eventually causes the crack to branch out, producing the roughest hackle region. The hackle region is characterized by elongated markings that emanate from the flaw origin [22]. These fracture phenomena are found in other brittle BMGs, such as Fe-based, Co-based, and Mg-based BMGs [23-25]. Zhang et. al. reported similar cleavage-fracture morphologies on fracture surfaces from compression tests on $Fe_{65.5}Cr_4Mo_4Ga_4P_{12}C_5B_{5.5}$ and $Co_{43}Fe_{20}Ta_{5.5}B_{31.5}$ [23]. They suggest (1) that the mirror morphology forms when the propagation velocity is lower than a critical velocity, (2) that the mist region is formed as the crack front accelerates toward a critical velocity, and (3) that the hackle region is formed when the crack exceeds a critical velocity and becomes unstable. They also found periodic, wavy nanoscale steps in the mirror, mist, and hackle regions, and suggested that these nanoscale steps enable the dynamic crack to dissipate more energy through a curving path [23]. Wang et. al. found an unusual fractographic evolution from a nanoscale, dimplelike structure to nanoscale periodic steps and corrugations, and then to a flat mirror zone along the crack-propagation direction when they conducted a three-point-bending test on $Mg_{65}Cu_{25}Gd_{10}$ BMG [25]. They propose that the transition is due to the propagation-speed dependent dynamic behavior of the viscoelastic matter at the crack-tip front, where local softening occurs in the fracture-process zone [25].

In the current study, no dimple-like structure or wavy corrugations were observed in the mirror and mist regions. However, periodic, wave-like nanoscale patterns were found in the hackle region, as shown in Figures 2(c) and 2(d). These periodic patterns suggest that the hackle ridges formed when the crack velocity or direction varied along the crack front [Figures 2(c) and 2(d)] [23]. In the mirror region, the crack velocity is low, and the crack front can keep the same

velocity. In the hackle region, the crack velocity is fast, and the propagation is unstable. Then the hackle ridges form. Figure 2(d) demonstrated that the periodic corrugations on both sides of a hackle ridge grew in different directions with asynchronous steps. The wavelength of the periodic corrugations is measured to be approximate 76 nm. The periodic nanoscale corrugations may result from a local plastic fracture, and the local plasticity plays a dominant role at the front of the crack tip [26]. However, these fine nanoscale patterns may reflect the relatively brittle fracture in BMGs.

The large-scale vein patterns and fine-scale wavy corrugations could be two indicators for the existence of the local ductility in the Ca-based BMG. In the present investigation, the vein patterns might result from the shear fracture through shear bands, which were generally observed in Zr and Cu-based BMGs, and the wavy corrugations were the results of splitting fracture through the crack-tip opening, which was usually found in Fe- and Co-based BMGs. This trend may indicate that the Ca-based BMG demonstrates different fracture characteristics. The Ca-based BMG has better local ductility under a shear-fracture mode than that under a splitting-fracture mode. Xi et. al. found that the plastic-process zone, *w*, (measured as the average width of the dimple or the wavelength of the vein features) increased linearly with the increase of $(K_C/\sigma_Y)^2$ where K_C is the fracture toughness, and σ_Y is the fracture strength [27]. We assume that the current Ca-based BMG follows the same trend. The average of σ_Y is about 364 MPa [15]. For the shear mode of the Ca-based BMG, *w* is up to 13.2 μm (estimated from the width of the dimple vein structure) and K_C is estimated to be ~ 8.79 MPa·m$^{0.5}$. For a splitting mode of the Ca-based BMG, *w* is 76 nm (estimated from the wavelength of the periodic steps/corrugations) and K_C is estimated to be ~ 0.75 MPa·m$^{0.5}$. Although the fracture toughness of the Ca-based BMG under shear mode can reach 8.79 MPa·m$^{0.5}$, the Ca-based BMG only exhibited very small

fracture toughness for splitting mode, which is comparable to the silicate glasses with K_C ~ 0.68 to 0.91 $MPa \cdot m^{0.5}$ [27]. This may suggest that the brittleness of the Ca-based BMG is close to common oxide glasses. Thus, the Ca-based BMG demonstrates two types of fracture behavior under the compression loading. In fact, it was found that the Poisson's ratio of the $Ca_{65}Mg_{15}Zn_{20}$ BMG is ~ 0.3 [3]. In general, metallic glasses with the Poisson's ratio less than 0.31 - 0.32 are more brittle [28]. Therefore, the current Ca-based BMG is in the transition from the "brittle" to "ductile" characteristics. The further investigation on the brittle/ductile fracture behavior of the Ca-based BMGs may provide an opportunity to thoroughly understanding the brittleness nature of BMGs.

CONCLUSIONS

The $Ca_{65}Mg_{15}Zn_{20}$ BMG exhibited the duality of fracture behavior under compression loading. SEM observation showed that the fracture surfaces contained the typical BMG vein pattern in the shear-fracture mode and the typical glass mirror, mist, and hackle patterns in the splitting/opening fracture mode. Furthermore, periodic nanoscale corrugations were found in the hackle region, which may indicate a local plasticity for the brittle fracture. Ca-based BMGs could be an ideal material for studying the brittle/ductile fracture mechanism in metallic glasses.

ACKNOWLEDGMENTS

We would like to acknowledge the financial support of the National Science Foundation: (1) the Division of the Design, Manufacture, and Industrial Innovation Program, under Grant No. DMI-9724476, (2) the Combined Research-Curriculum Development (CRCD) Programs, under EEC-9527527 and EEC-0203415, (3) the Integrative Graduate Education and Research Training

(IGERT) Program, under DGE-9987548, (4) the International Materials Institutes (IMI) Program, under DMR-0231320, (5) the Major Research Instrumentation (MRI) Program, under DMR-0421219, (6) the Division of Civil, Mechanical, Manufacture, and Innovation Program, under CMMI-0900271, and (7) the Materials World Network Program, under DMR-00909037, with Ms. M. Poats, and Drs. C. V. Hartesveldt, D. Dutta, P. W. Jennings, L. S. Goldberg, L. Clesceri, C. Huber, C. E. Bouldin, Dr. C. V. Cooper, and Dr. A. Ardell as contract monitors. Work at the Air Force Research Laboratory (AFRL) was conducted through the AFRL on-site contract No. FA8650-10-D-5226 and through an AFOSR Task (01ML05-COR, Dr. J. Fuller, Program Manager).

REFERENCES

O. N. Senkov, D. B. Miracle, and J. M. Scott, Intermetallics 14, 1055 (2006).

M. L. Morrison, R. A. Buchanan, O. N. Senkov, D. B Miracle, and P. K. Liaw, Metallurgical and Materials Transactions A 37, 1239 (2006).

O. N. Senkov, D. B. Miracle, V. Keppens, and P. K. Liaw, Metallurgical and Materials Transactions A 39A, 1888 (2008).

K. Amiya and A. Inoue, Mater. Trans. JIM 43, 81 (2002).

K. Amiya and A. Inoue, Mater. Trans. JIM 43, 2578 (2002).

O. N. Senkov and J. M. Scott, Mater. Lett. 58, 1375 (2004).

O. N. Senkov and J. M. Scott, Scripta Mater. 50, 449 (2004).

F. Q. Guo, S. J. Poon, and G. J. Shiflet, Appl. Phys. Lett. 84, 37 (2004).

O. N. Senkov and J. M. Scott, Journal of Non-Crystalline Solids 351, 3087 (2005).

E. S. Park, W. T. Kim, and D. H. Kim, Mater. Sci. Forum 475-479, 3415 (2005).

O. N. Senkov, J. M. Scott, and D. B. Miracle, Journal of Alloys and Compounds 424, 394 (2006).

S. Gorsse, G. Orveillon, O. N. Senkov, and D. B. Miracle, Physical Review B 73, 224202 (2006).

M. D. Demetriou, A. Wiest, D. C. Hofmann, W. L. Johnson, B. Han, N. Wolfson, G. Y. Wang, and P. K. Liaw, JOM 62, 83 (2010).

C. A. Schuh, T. C. Hufnagel, and U. Ramamurty, Acta Materialia 55, 4067 (2007).

G. Y. Wang, P. K. Liaw, O. N. Senkov, D. B. Miracle, and M. L. Morrison, Advanced Engineering Materials 11, 27, (2009).

J. Raphael, G. Y. Wang, P. K. Liaw, O. N. Senkov, and D. B. Miracle, "Fatigue and Fracture Behavior of a Ca-Based Bulk-Metallic Glass", Metallurgical and Materials Transactions A (2010), in press.

J. J. Lewandowski and A. L. Greer, Nature Materials 5, 15 (2006).

B. Yang, C. T. Liu, T. G. Nieh, M. L. Morrison, P. K. Liaw, and R. A. Buchanan, J. Mater. Res. 21, 915 (2006).

Z. F. Zhang, J. Eckert, and L. Schultz, Acta Materialia 51, 1167 (2003).

H. Li, C. Fan, K. Tao, H. Choo, and P. K. Liaw, Advanced Materials 18, 752 (2006).

W. H. Jiang, G. J. Fan, H. Choo, and P. K. Liaw, Materials Letters 60, 3537 (2006).

J. J. Mecholsky, S. W. Freiman, and R. W. Rice, Journal of Materials Science 11, 1310 (1976).

Z. F. Zhang, F. F. Wu, W. Gao, J. Tan, Z. G. Wang, M. Stoica, J. Das, J. Eckert, B. L. Shen, and A. Inoue, Applied Physics Letters 89, 251917 (2006).

G. Wang, Y. T. Wang, Y. H. Liu, M. X. Pan, D. Q. Zhao, and W. H. Wang, Applied Physics Letters 89, 121909 (2006).

G. Wang, Y. N. Han, X. H. Xu, F. J. Ke, B. S. Han, and W. H. Wang, Journal of Applied Physics 103, 093520 (2008).

G. Wang, D. Q. Zhao, H.Y. Bai, M. X. Pan, A. L. Xia, B. S. Han, X. K. Xi, Y. Wu, and W. H. Wang, Physical Review Letters 98, 235501 (2007).

X. K. Xi, D. Q. Zhao, M. X. Pan, W. H. Wang, Y. Wu, and J. J. Lewandowski, Physical Review Letters 94, 125510 (2005).

J. J. Lewandowski, W. H. Wang, and A. L. Greer, Philosophical Magazine Letters 85, 77 (2005).

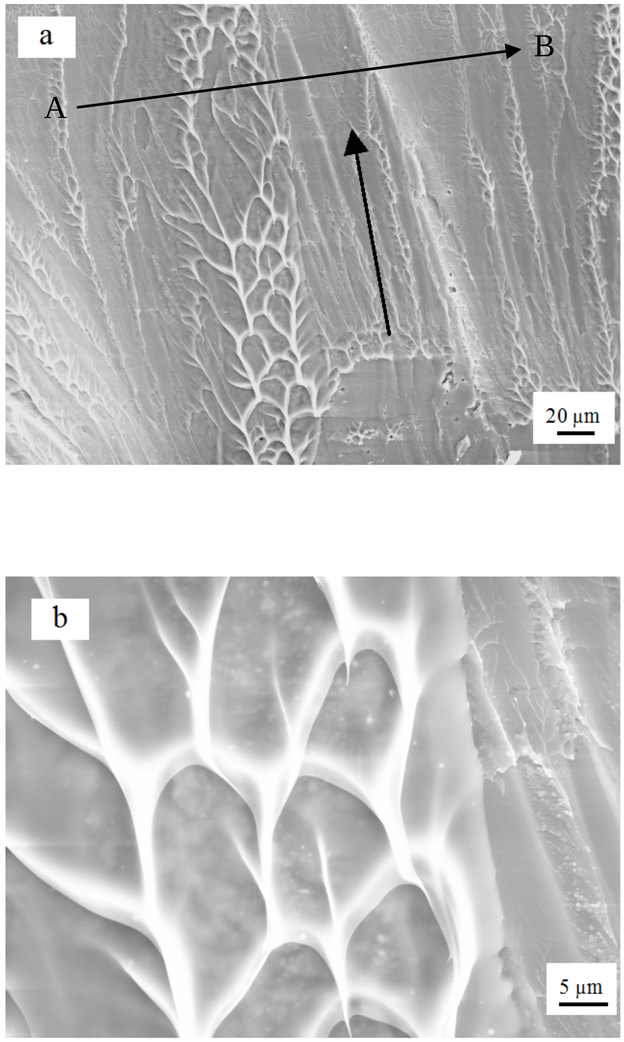

Figure 1. Vein patterns in the shear fracture surface of the $Ca_{65}Mg_{15}Zn_{20}$ BMG after a compression experiment (a) at a lower magnification and (b) at a higher magnification. The solid arrows indicate the crack-growth directions.

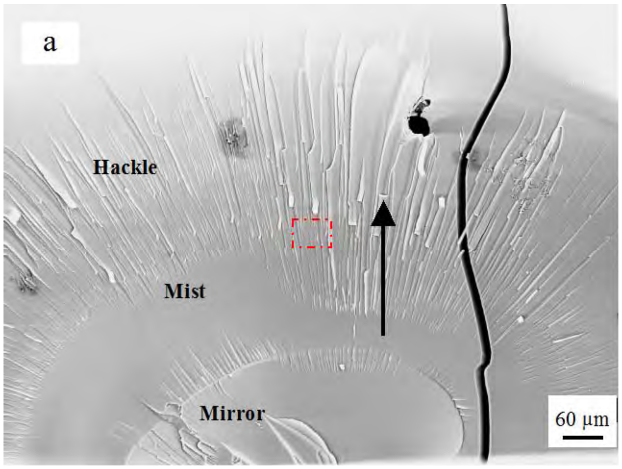

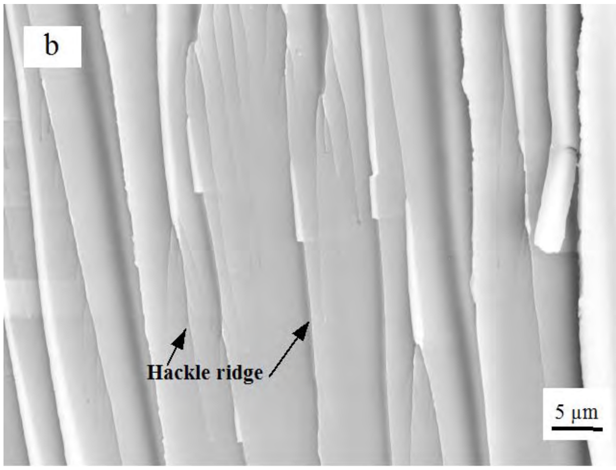

Figures 2a and 2b

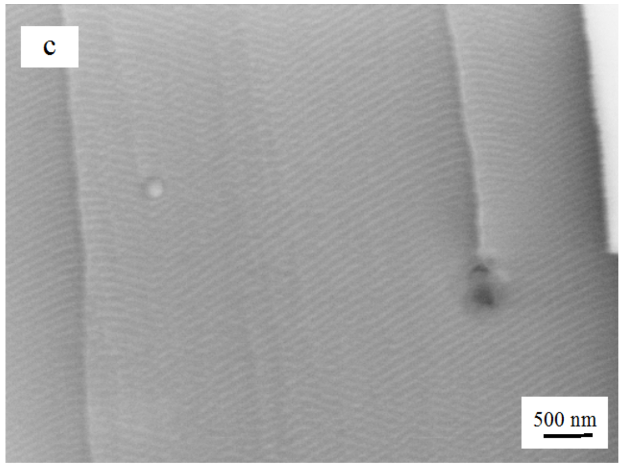

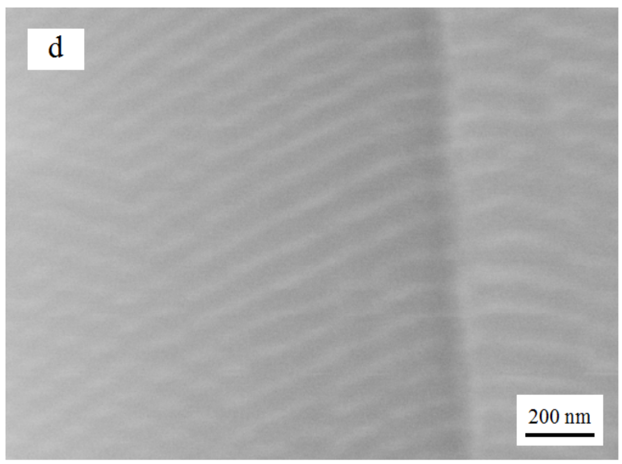

Figure 2. Fracture-surface morphology on the splitting surface of the $Ca_{65}Mg_{15}Zn_{20}$ BMG after a compression experiment. (a) Brittle fractography with mirror, mist, and hackle morphologies. (b) Detailed morphology of the hackle zone inside the box in (a). (c) and (d) Periodic corrugations at a higher magnification. The solid arrows indicate the crack-growth direction.